Simulation of electromechanical responses of ferroelectric ceramics driven by alternating compressive stress and static electric field

Simon Ching-kin Chow[a] and Veng-cheong Lo
Department of Applied Physics, The Hong Kong Polytechnic University, Hung Hom, Kowloon, Hong Kong, China

(Received 30 July 2008; accepted 7 October 2008; published online 19 November 2008)

The effect of static electric field on mechanical and dielectric properties of a lead zirconate titanate ($PbZr_xTi_{1-x}O_3$) piezoceramic sample driven by an alternating compressive stress has been experimentally investigated by Zhou *et al.* [J. Am. Ceram. Soc. **88**, 867 (2005)]. Numerical simulation for this experimental result using two-dimensional four-state Potts model is presented in this article. Upon polarization switching, the dipole in the perovskite cell undergoes 90° rotation, which is in turn associated with the switching of ferroelastic strain state. Consequently, the stress-strain relation and hence the mechanical stiffness are strongly influenced by the magnitude of the dc bias. Optimal mechanical and piezoelectric responses can be obtained by the suitable selection of biasing field. © *2008 American Institute of Physics*. [DOI: 10.1063/1.3026537]

I. INTRODUCTION

Perovskite-type ferroelectrics such as lead zirconate titanate (PZT) and barium titanate ($BaTiO_3$) are widely used for the applications of electromechanical devices such as sensors and actuators due to their large electromechanical coupling effect and high permittivity. Typical examples include buzzers, telephone diaphragms, surface acoustic wave filters, and ultrasonic cleaner. Mostly these materials are in ceramic forms. The performance of these piezoceramics is sensitive to the loading conditions, which demands a thorough study under various loading conditions. For instance, a piezoceramic device driven by a high-frequency and low-amplitude electric field demonstrates linear electromechanical responses,[1–5] which can be expressed by a pair of linear constitutive relations. However, under the condition of large amplitude and low frequency, the corresponding piezoelectric, elastic, and dielectric properties show nonlinear and hysteretic behaviors. This situation becomes prominent where a large output signal is required, such as precision positioning devises, noise controls, and automotive sensors. There have been continuous efforts to pursue a theoretical explanation for this nonlinearity.[1,2,4,6–10] For example, Kamlah[4] and Landis[10] reviewed different theoretical approaches responsible for the nonlinear electromechanical responses.

Regarding the influence of loading conditions, it has been suggested that, by a suitable combination of electrical and mechanical loadings, an optimal performance can be achieved. There are basically three combinations for the electrical and mechanical loadings: (1) alternating electric field and static stress, (2) alternating stress and dc field, and (3) both alternating field and stress with an arbitrary phase difference. Lynch,[11] Chaplya,[12] and Zhou *et al.*[5] studied the effect of static stress on the polarization and strain of a PZT ceramic driven by an alternating electric field. They observed that both the remanent polarization and spontaneous strain are suppressed under a large longitudinal compressive stress. Moreover, the area of the strain-electric field (ε-E) butterfly loop is enhanced by the compressive stress of moderate amplitude. On the other hand, Zhou *et al.*[13] investigated the effect under both alternating compressive stress and field. Both the stress and field were of the same frequency but at different phases. It is observed that the phase difference is an important factor for the electromechanical responses. Under the in-phase condition, both polarization versus electric field (P-E) and longitudinal strain versus electric field (ε-E) loops are suppressed but they are enhanced under the out-of-phase condition. This novel behavior has been explained by the ferroelastic/ferroelastic switching through the domain wall movements predominantly contributed by 90° rotations of dipoles.[14] As many are interested in the effect of mechanical loading on the ferroelectric and dielectric properties, few have paid attention to the effect of static electric field on the mechanical properties. The latter is related to an important issue of electric field–dependent mechanical stiffness, which is useful in many different smart material designs. Zhou *et al.*[5] investigated the stress-strain (σ-ε) and stress–electric displacement (σ-D) relations under different static electric fields. They attributed their observations to the non-180° domain switching.

It has been established that there are two major contributions responsible for both the dielectric and electromechanical properties: intrinsic and extrinsic contributions. The former is due to the charge separation between ions and is the only contribution for a single-domain sample. The latter involves the domain wall movements, which are associated with the rotations of dipoles near the domain walls. The rotations can be classified into two kinds: 180° and non-180°. Kim *et al.*[15] discussed the importance of extrinsic contribution. They utilized the temperature dependence of the intrinsic contribution and determined its contribution to the permittivity with different Zr/Ti ratios near absolute zero temperature. The extrinsic contribution was then obtained from subtracting the total permittivity by the temperature-

[a]Electronic mail: simon.ckchow@gmail.com.

dependent intrinsic contribution. They concluded that the extrinsic contribution is dominant. Furthermore, it has been established that only the non-180° dipolar rotation is associated with the piezoelectric effect.[3,5,10,12,16] Consequently, it is necessary to incorporate non-180° dipolar rotations in order to simulate the electromechanical properties of PZT-based materials.

In this paper, we present the simulation result for the effect of a static electric field on the stress-strain relation of PZT-based ferroelectrics using a four-state Potts model. In Sec. II, the theoretical model and assumptions are presented. In Sec. III, the simulation results are presented and compared with experiments.

II. THEORY AND MODELING

For a PZT ferroelectric solid in tetragonal phase, the majority of electromechanical response is caused by the 90° dipolar switching,[1–5,12,13,17] and four is the minimal number of states to simulate the electromechanical effects using Monte Carlo method. The sample is modeled by a multidomained single crystalline system. The direction of c-domain is along the z-axis, which is also denoted as (001) or "3" direction, while that of a-domain is either along x axis [(100) or "1" direction] or y axis [(010) or "2" direction]. Because of the equivalence between the two transverse directions, the system can be simplified into a two-dimensional one lying on the xz plane. The size of the system is $N_x \times N_z$, where N_x and N_z are the numbers of cells along the x and z directions, respectively. The dipole moment of a cell can be represented by a pseudospin matrix $\hat{S}_{ij}$, where i and j are indices to represent the position of the cell and $0 \le i \le N_x$ and $0 \le j \le N_z$. There are four possible states for each of these pseudospins. Moreover, the pseudospin state is associated with the distortion of the same perovskite cell.[14] The latter is denoted by the ferroelastic strain matrix $\hat{\varepsilon}^F_{ij}$. The four different states of the pseudospin matrix and their associated ferroelastic strain states are defined as follows:

$$\hat{S}_A = \begin{pmatrix} 1 \\ 0 \end{pmatrix} \quad \text{and} \quad \hat{\varepsilon}^F_c = \begin{pmatrix} \varepsilon_0 \\ -\varepsilon_0/2 \end{pmatrix} \quad (\text{along the } +z \text{ direction}),$$

$$\hat{S}_B = \begin{pmatrix} 0 \\ 1 \end{pmatrix} \quad \text{and} \quad \hat{\varepsilon}^F_a = \begin{pmatrix} -\varepsilon_0 \\ \varepsilon_0/2 \end{pmatrix} \quad (\text{along the } +x \text{ direction}),$$

$$\hat{S}_C = \begin{pmatrix} -1 \\ 0 \end{pmatrix} \quad \text{and} \quad \hat{\varepsilon}^F_c = \begin{pmatrix} \varepsilon_0 \\ -\varepsilon_0/2 \end{pmatrix} \quad (\text{along the } -z \text{ direction}),$$

$$\hat{S}_D = \begin{pmatrix} 0 \\ -1 \end{pmatrix} \quad \text{and} \quad \hat{\varepsilon}^F_a = \begin{pmatrix} -\varepsilon_0 \\ \varepsilon_0/2 \end{pmatrix} \quad (\text{along the } -x \text{ direction}), \tag{1}$$

where ε_o is a constant strain value. In addition to the ferroelastic strain, there are two more strain components: elastic and field-induced ones. The elastic strain is related to the stress by the following relation:

$$\hat{\varepsilon}^{el}_{ij} = \begin{pmatrix} \varepsilon^{el}_3 \\ \varepsilon^{el}_1 \end{pmatrix} = \frac{1}{Y} \begin{pmatrix} 1 & -\nu \\ -\nu & 1 \end{pmatrix} \begin{pmatrix} \sigma_3 \\ \sigma_1 \end{pmatrix}, \tag{2}$$

where Y and ν are, respectively, the Young's modulus and Poisson ratio. Unlike the ferroelastic strain caused by the rotation of dipole, the field-induced strain $\hat{\varepsilon}^{EI}_{ij}$ is induced by the charge separation in the presence of electric field. The longitudinal (3) and the transverse (1) components are related to the electric field by the following expressions:

$$(\varepsilon^{EI}_3)_{ij} = d_{33}E_3 + d_{31}E_1 + q_{333}E_3^2 + q_{313}E_1E_3 + q_{331}E_3E_1 + q_{311}E_1^2,$$

$$(\varepsilon^{EI}_1)_{ij} = d_{13}E_3 + d_{11}E_1 + q_{133}E_3^2 + q_{113}E_1E_3 + q_{131}E_3E_1 + q_{111}E_1^2, \tag{3}$$

where d_{mk} and q_{mkl} are the "piezoelectric" and "electrostriction" tensors, respectively; m and $k = 1$ or 3. By the symmetry property, $d_{13} = d_{31}$, $q_{113} = q_{311} = q_{131}$, and $q_{313} = q_{133} = q_{331}$. Moreover, when the applied field is small, the quadratic terms are negligible. The total strain is the summation of these three contributions, so that

$$\hat{\varepsilon}_{ij} = \hat{\varepsilon}^F_{ij} + \hat{\varepsilon}^{el}_{ij} + \hat{\varepsilon}^{FI}_{ij}. \tag{4}$$

The system Hamiltonian is given by

$$H = -\sum_{i,j,k,l} J\{\hat{S}^T_{ij}\hat{S}_{kl}\} - P_S \sum_{i,j} \{\hat{E}^T_{ij}\hat{S}_{ij}\} - \sum_{ij} \hat{\sigma}^T_{ij}\hat{\varepsilon}_{ij} - \alpha \sum_{i,j,k,l} \hat{\varepsilon}^{F^T}_{ij}\hat{\varepsilon}^F_{kl} + H', \tag{5}$$

where J is the coupling coefficient between neighboring dipoles and $\hat{X}^T$ is the transpose matrix of the generic matrix $\hat{X}$. The expression enclosed by the curly brace $\{\ldots\}$ denotes the matrix product. P_S is the saturation polarization and α is the coupling coefficient between neighboring ferroelastic strain states. $\hat{E}_{ij}$ and $\hat{\sigma}_{ij}$ are the matrix representations of electric field and stress, respectively. H' accounts for the anisotropic effect characterized by an anisotropic switching factor ϕ_C, which is the energy barrier for a dipole switching from a-domain to c-domain. The physical meaning for this term has been discussed previously.[14] It should be noted that each of the terms in Eq. (5) is in unit of energy density (J m^{-3}).

From the experiment of Zhou *et al.*,[3] the sample was prepoled along negative z-axis. In our simulation, this prepoled sample consists of domains oriented over all the four directions resulting in a net polarization along negative z-axis. The poling is implemented by applying a constant E field. Ensembles of pseudospins and ferroelastic matrices are then obtained and are treated as the initial conditions for our simulation. A longitudinal compressive stress with triangular waveform is then applied. It varies from 0 to 400 MPa at a rate of 5 MPa/s under static electric fields of different amplitudes. The stress is then released to 0 MPa at the same rate. At every Monte Carlo step, the change in Hamiltonian ΔH is evaluated. The ensembles of pseudospins $\{\hat{S}_{ij}\}$ and ferroelas-

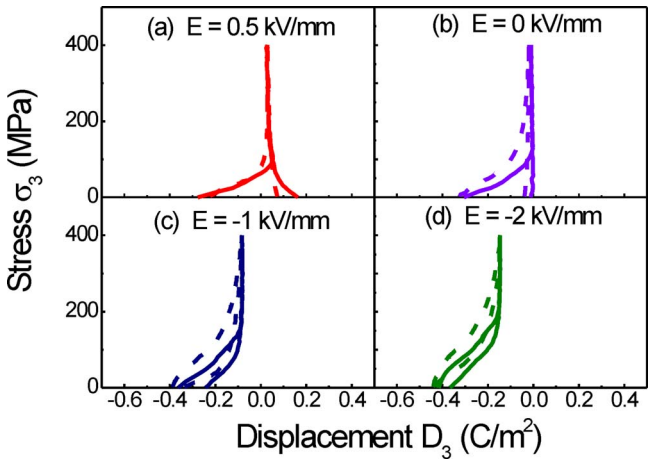

FIG. 1. (Color online) σ_3-D_3 loops under different dc biasing conditions: (a) +5.0, (b) 0.0, (c) −1.0, and (d) −2.0 kV/mm, respectively. Simulation results are denoted by solid lines and experimental ones by dotted lines.

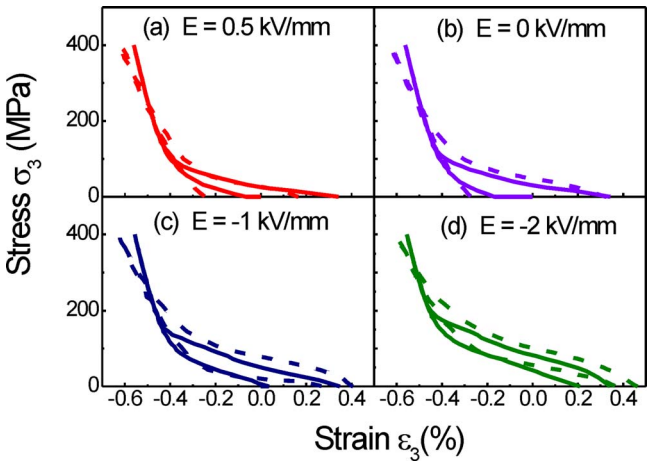

FIG. 2. (Color online) σ_3-ε_3 relations under different dc biasing conditions: (a) +5.0, (b) 0.0, (c) −1.0, and (d) −2.0 kV/mm, respectively. Simulation results are denoted by solid lines and experimental ones by dotted lines.

tic strain states $\{\hat{\varepsilon}_{ij}^F\}$ are then updated according to the METROPOLIS algorithm.

The overall longitudinal polarization and strain of the sample are calculated by the following relations:

$$P_3 = \frac{P_s \sum_{ij} \{\hat{n}^T \hat{S}_{ij}\}}{N_x N_z}, \tag{6}$$

$$\varepsilon_3 = \frac{1}{N_x N_z} \sum_{ij} \hat{n}^T (\hat{\varepsilon}_{ij} - \hat{\varepsilon}_{ij}^0), \tag{7}$$

where $\hat{\varepsilon}_{ij}^0$ is the initial strain matrix for each cell, and $\hat{n} = \binom{1}{0}$ is the longitudinal unit matrix. The electric displacement D_3 can be obtained by the constitutive equation as follows:

$$D_3 = \kappa_0 E_3 + P_3 + d_{3m}\sigma_m, \tag{8}$$

where κ_o and d_{3m}, are, respectively, the dielectric permittivity in free space and piezoelectric coefficient of the whole sample. The stress σ_m is a second rank stress tensor with the index $m=1$, 3, and 5 representing 11, 33, and 13 components.[16] The calculated electric displacement vector and strain against stress for different dc biasing fields are obtained and compared with the experimental results reported by Zhou *et al.*[3]

III. RESULTS AND DISCUSSION

The numerical parameters for this simulation are: the amplitude and period of the alternating compressive stress 400 MPa and 160 s, Young's modulus$=2.59\times10^{11}$ Pa, Poisson ratio$=0.3$, $P_s=0.557$ C m^{-2}, piezoelectric coefficients d_{33} of a dipole$=2.61\times10^{-11}$ C N^{-1} and $d_{31}=-2.1\times10^{-10}$ C N^{-1}, temperature $T=300$ K, anisotropic energy barrier $h_3=5.56\times10^5$ J m^{-3}, $\phi_C=0.45$, $q_{113}=q_{311}=q_{131}=q_{313}=q_{133}=q_{331}\cong0$, $N_x=150$, $N_z=80$, and $J=4.5\times10^5$ J m^{-3}. The variations in electrical displacement D_3 and mechanical strain ε_3 over a complete cycle of compressive stress loading σ_3 and under different dc biasing conditions (+0.2, 0.0, −0.2, and −0.4 kV/mm) are shown in Figs. 1 and 2, respectively. In these graphs, the simulation results are represented by solid lines and the experimental ones obtained from Zhou *et al.*[3] are in dotted lines. The agreement between theory and experiment is satisfactory.

The presence of a static electric field strongly influences the switching of dipoles, as manifested by the different σ_3-D_3 and σ_3-ε_3 loops. Figures 3 and 4 depict the effect of biasing field on these curves. Labels α, β, χ, and δ on these two figures represent the four different stages at 0, 100, 200, and 300 MPa, respectively. The corresponding domain configurations are illustrated in Fig. 5. In the absence of any dc bias, only the down domain exists at stage α, as the sample has been negatively poled. At β, the presence of compressive stress cancels out some of the field-induced strain, which initially exists. Consequently, the longitudinal size shrinks while the transverse one expands. Both σ_3-D_3 and σ_3-ε_3 relations are linear for small stress, due to the elastic response. At χ, the compressive stress exceeds a threshold value, most of the dipoles inside a domain acquire enough energy to perform 90° rotation. This leads to abrupt and nonlinear changes in strain and electrical displacement. At δ, a tremendous number of dipoles switch from longitudinal to trans-

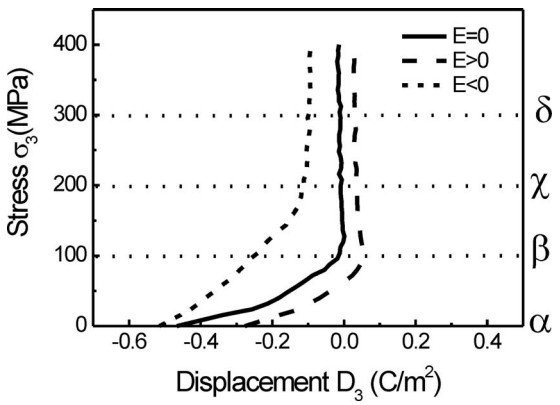

FIG. 3. σ_3-D_3 relations during the loading period with σ_3 increasing from 0 to 400 MPa under different dc biasing conditions (solid line: field free, dash line: positive bias, and dotted line: negative bias). The labels α, β, χ, and δ are the stages when the stress level reaches 0, 100, 200, and 300 MPa, respectively.

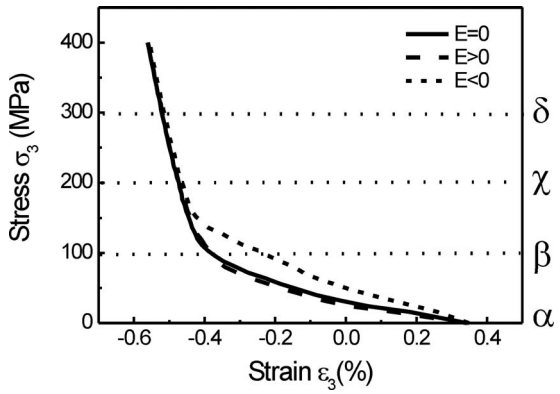

FIG. 4. σ_3-ε_3 relations during the loading period with σ_3 increasing from 0 to 400 MPa under different dc biasing conditions (solid line: field free, dash line: positive bias, and dotted line: negative bias).

verse direction through 90° rotation. *a*-domains in both states B and C dominate. There is little change in electrical displacement and a slight but linear change in strain due to the purely elastic effect.

In the presence of a negative biasing field, the sample starts with a larger longitudinal strain and a larger negative electrical displacement due to the presence of field induced strain. At stages α and β, the application of a small compressive stress reduces the longitudinal size without the rotation of dipoles, resulting in linear σ_3-D_3 and σ_3-ε_3 relations. It should be noted that a larger coercive stress is required to enable dipole rotations. On further increasing the compressive stress at stage χ, a tremendous number of dipoles rotate toward the two transverse directions. Finally, at δ, it exhibits a vertical σ_3-D_3 and a linear σ_3-ε_3 relations as in the field-free case. On the other hand, in the presence of a positive biasing field, the sample starts with a smaller strain and negative displacement due to the reduction in longitudinal length of the sample. Moreover, the positive biasing field encourages 90° dipolar rotation, as manifested by a smaller coercive stress. Furthermore, some dipoles even switch to state A (along $+z$ direction), increasing the electrical displacement. The further increase in compressive stress forces most of the dipoles to be aligned along the transverse directions, resulting in a slight decrease in electrical displacement. The latter then maintains a constant value and exhibits a

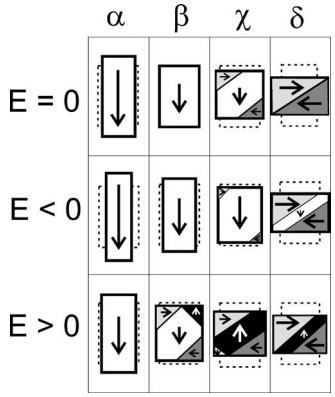

FIG. 5. Domain configurations at different stages of compressive stress loading. The dotted rectangle shows the original undistorted sample for reference purposes.

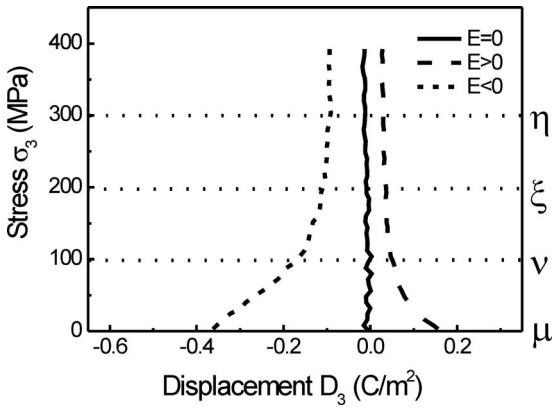

FIG. 6. σ_3-D_3 relations during the unloading period with σ_3 decreasing from 400 to 0 MPa under different dc biasing conditions (solid line: field free, dash line: positive bias and dotted line: negative bias). The labels μ, ν, ξ, and η are the stages when the stress level decreases to 300, 200, 100, and 0 MPa, respectively.

vertical stress-displacement relation as in all other biasing cases. The vertical stress-displacement relations at large compressive stress are nearly parallel for different biasing fields. The difference in displacement values at different dc biases is mainly due to the linear dielectric effect.

σ_3-D_3 and σ_3-ε_3 relations during the unloading of compressive stress from 400 to 0 MPa are shown in Figs. 6 and 7, respectively. The corresponding domain configuration is sketched in Fig. 8. The labels η, ξ, ν, and μ correspond to the stages when the compressive stress is reduced to 300, 200, 100, and 0 MPa, respectively. The relaxation of domain configuration is strongly influenced by the biasing field and the built-in stress. This built-in stress was induced during the sample preparation. For instance, in the field-free case, the electrical displacement is restored to a small negative value and a negative residual strain exists. The σ_3-D_3 curve is nearly vertical, except with a slight bending toward the negative displacement direction. It is obviously caused by a small longitudinal residual stress. For a negative biasing condition, some of the transverse domains will be restored to the longitudinal ones (in state C). This induces a large amount of 90° ferroelastic switching. Finally, it attains a large negative displacement. Under a positive bias, however, the 90° ferroelastic switching drives the dipoles into state A, resulting in a slight positive displacement value.

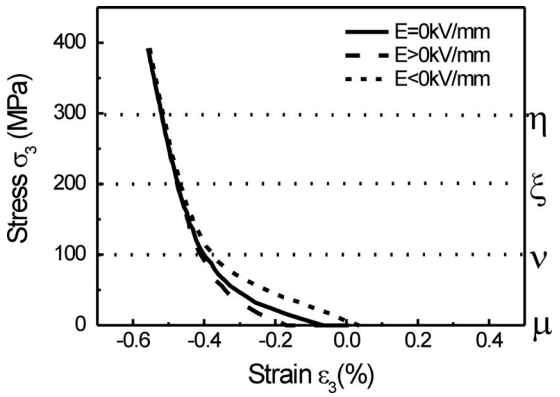

FIG. 7. σ_3-ε_3 relations during the unloading period with σ_3 decreasing from 400 to 0 MPa under different dc biasing conditions (solid line: field-free, dash line: positive bias, and dotted line: negative bias).

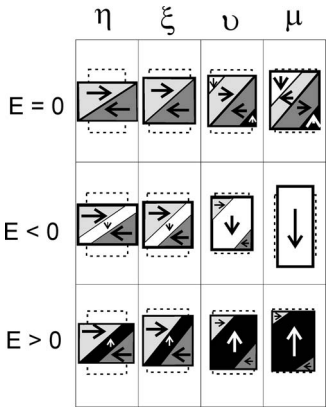

FIG. 8. Domain configurations at different stages of unloading, the compressive stress, and different biasing conditions.

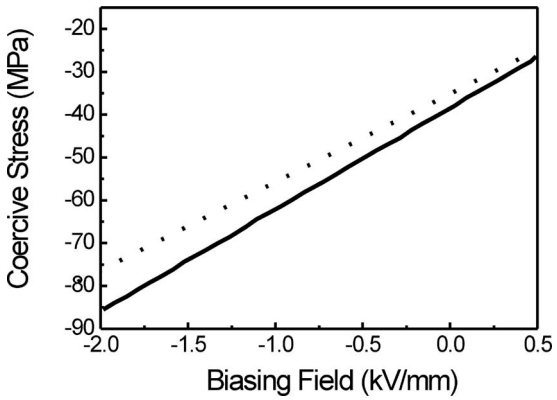

FIG. 10. Comparison of computed (dotted line) and experimental (solid line) coercive stress against biasing field.

For the mechanical behavior, different biasing fields give rise to different final strain values. The more negative bias is applied, the larger the positive strain is obtained. This is an inverse piezoelectric effect. Like the σ_3-D_3 curve, there is also a linear region in each of the stress-strain curve under a small compressive stress, followed by an inflection point on increasing the compressive stress. This inflection point reflects a tremendous ferroelastic switching of dipoles, giving rise to a rapid increase in (compressive) strain magnitude. On further increasing the compressive stress, σ_3-ε_3 curves of different biasing conditions converges into a straight line. The latter is due to the purely elastic response. During the unloading process, the strain drops linearly in the field-free and positive biasing cases, reflecting that there is no appreciable ferroelastic switching toward the longitudinal direction. On the other hand, a large negative biasing field can trigger tremendous ferroelastic switching, leading to a larger longitudinal (tensile) strain.

The variations in compliance s_{33} and piezoelectric coefficient d_{33} against stress σ_3 during the stress loading period from 0 to 400 MPa are shown in Fig. 9. Each curve corresponds to a constant dc biasing field. The dynamic compliance and piezoelectric coefficient are calculated by $\partial\varepsilon_3/\partial\sigma_3$ and $\partial D_3/\partial\sigma_3$, respectively, using forward Euler estimation.

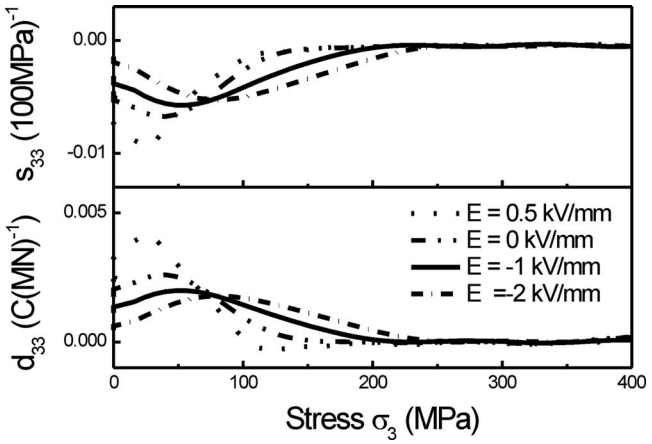

FIG. 9. Computed mechanical compliance s_{33} (above) and piezoelectric coefficient d_{33} (below) against compressive stress magnitude under different biasing fields: 0.5 (dotted), 0 (dash-dot-dot), −1 (solid), and −2 kV/mm (short dash-dot).

Each of the s_{33}-σ_3 and d_{33}-σ_3 curves is nonlinear and exhibits a peak at a specific stress magnitude. Both the peak position and height depend on the biasing field. In particular, the positive biasing field gives rises to both largest s_{33} and d_{33} values.

Due to the negative poling, all dipoles are supposed to be initially at state C. The application of a small compressive stress on one hand reduces the longitudinal size of the sample and hence of the individual cells. On the other hand, it can also drive the dipoles to state B or D, undergoing ferroelastic switching by 90° rotations. This is called the subcoercive switching. Both the piezoelectric coefficient and mechanical compliance increase with the stress magnitude, until the latter reaches the coercive stress value. At this value, a tremendous number of dipoles undergo ferroelastic switching. On further increasing the stress magnitude, the number of dipoles being at the transverse directions increases and those switchable ones are reduced. Consequently, both the piezoelectric coefficient and mechanical compliance decrease to zero at large stress magnitude. Moreover, there is no sharp critical point separating the two mechanisms: shrinkage of longitudinal dimensional and 90° rotation of dipoles.

With all dipoles initially at state C, the presence of a positive electric field assists 90° rotations and drives them to states B or D or even to state A. This will reduce the coercive stress. Moreover, because the number of switchable dipoles is large when the compressive stress increases from zero to the coercive value, there is a drastic change in strain and electrical displacement. It results in both maximum piezoelectric coefficient and mechanical compliance.

On a contrary, the negative dc bias helps the dipoles at state C to resist the ferroelastic switching driven by the compressive stress. Consequently, there is a wider range of stress where subcoercive switching takes place. The coercive stress is attained at a much larger stress magnitude. At the coercive stress, the number of switchable dipoles is reduced, resulting in smaller piezoelectric coefficient and mechanical compliance.

The coercive stresses, both computed by this simulation and determined from experiment of Zhou *et al.*,[3] are shown in Fig. 10. It is revealed that both of them are monotonically increasing with the biasing field. Furthermore, the theoretical

value is larger than the experimental one at the same applied field. The major reason is that the experimental values were actually measured from a polycrystalline sample but the simulation results are computed from a single crystalline system. Due to the random orientation of grains, the initial poling does not force all dipoles into state C of their corresponding grains.[18]

IV. CONCLUSION

The effects of dc biasing field on the strain and electrical displacement of a prepoled PZT sample driven by a cyclic compressive stress have been numerically simulated using the Monte Carlo simulation. The result demonstrates that both the dielectric and mechanical responses are strongly influenced by the biasing field. The latter can either assist or impede the ferroelastic switching induced by compressive stress, depending on the sign of the electric field. The abrupt and nonlinear stress-strain and stress–electrical displacement relations are caused by the onset of ferroelastic switching. The piezoelectric coefficient and mechanical compliance are also determined. It is found that both parameters can be maximized by the application of a positive biasing field.

ACKNOWLEDGMENTS

This work is financially supported by the Research Grant No. PolyU 5010/07P from the Hong Kong Polytechnic University.

[1] J. Huber, N. Fleck, and R. McMeeking, Ferroelectrics **228**, 39 (1999).
[2] C. Landis and R. McMeeking, Ferroelectrics **255**, 13 (2001).
[3] D. Zhou, M. Kamlah, and D. Munz, J. Am. Ceram. Soc. **88**, 867 (2005).
[4] M. Kamlah, Continuum Mech. Thermodyn. **13**, 219 (2001).
[5] D. Zhou, M. Kamlah, and D. Munz, J. Eur. Ceram. Soc. **25**, 425 (2005).
[6] S. Hwang, J. Huber, R. McMeeking, and N. Fleck, J. Appl. Phys. **84**, 1530 (1998).
[7] S. Hwang and R. McMeeking, Ferroelectrics **211**, 177 (1998).
[8] S. Hwang and R. McMeeking, Int. J. Solids Struct. **36**, 1541 (1999).
[9] S. Klinkel, Int. J. Solids Struct. **43**, 7197 (2006); V. C. Lo, J. Appl. Phys. **92**, 6778 (2002).
[10] C. Landis, Curr. Opin. Solid State Mater. Sci. **8**, 59 (2004).
[11] C. Lynch, Acta Mater. **44**, 4137 (1996).
[12] P. Chaplya and G. Carman, J. Appl. Phys. **90**, 5278 (2001).
[13] D. Zhou and M. Kamlah, J. Appl. Phys. **96**, 6634 (2004).
[14] V. C. Lo, W. Chung, and S. Chow, J. Appl. Phys. **101**, 114111 (2007).
[15] D. Kim, J. Maria, S. Kingon, and S. Streiffer, J. Appl. Phys. **93**, 5568 (2003).
[16] K. Uchino, *Ferroelectric Devices* (Marcel Dekker Inc., New York, 2000).
[17] D. Bolten, U. Bottger, and R. Waser, J. Eur. Ceram. Soc. **24**, 725 (2004).
[18] T. Kamel and G. With, J. Eur. Ceram. Soc. **28**, 1827 (2008).